

# TI Designs: TIDA-01054

## 用于消除高性能 DAQ 系统中的 EMI 影响的多轨电源参考设计



### 说明

借助于 LM53635-Q1 降压转换器，该参考设计可帮助消除 EMI 对高于 16 位的数据采集 (DAQ) 系统造成的性能下降影响。借助该降压转换器，设计人员可以将电源解决方案放置在靠近信号路径的位置，而不会产生不必要的 EMI 噪声降级，同时可以节省布板空间。该设计使用 20 位 1MSPS SAR ADC 支持 100.13dB 的系统 SNR 性能，这基本匹配使用外部电源时的 100.14dB SNR 性能。

### 资源

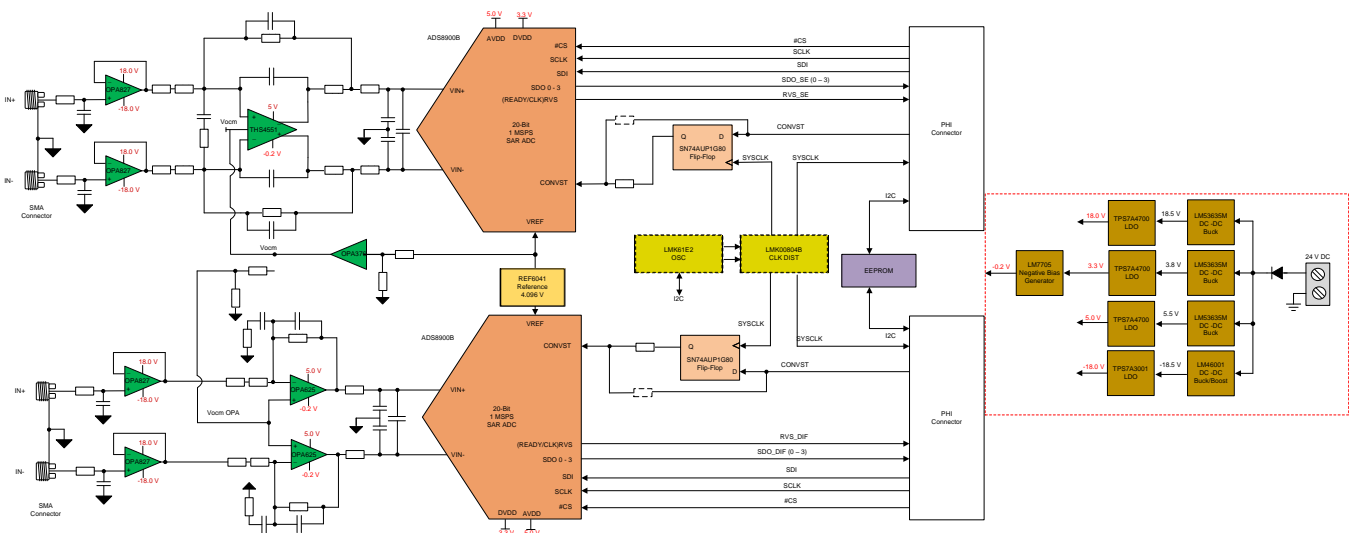
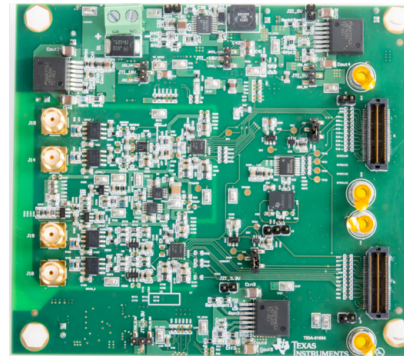
- TIDA-01054 设计文件夹
- LM53635-Q1 产品文件夹
- LM5574、LM46001、TPS7A3001 产品文件夹
- TPS7A47、LM7705 产品文件夹
- SN74AHC1G04、SN74AUP1G80 产品文件夹
- LMK61E2、LMK00804B 产品文件夹
- OPA827、OPA625、THS4551 产品文件夹
- REF6041 产品文件夹

### 特性

- 电源设计可最大程度地减小直流/直流 EMI 对系统性能的影响
- 具有两个 20 位 SAR ADC 通道
- 适用于可重复的高通道数系统的模块化前端参考设计
- 高达  $\pm 4V$  的输入信号 (8V<sub>PP</sub> 差动)

### 应用

- 数据采集 (DAQ)
- 半导体测试设备
- LCD 测试设备
- 实验室仪表
- 电池测试



Copyright © 2017, Texas Instruments Incorporated



该 TI 参考设计末尾的重要声明表述了授权使用、知识产权问题和其他重要的免责声明和信息。

## 1 System Description

Multi-input systems requiring the simultaneous or parallel sampling of many data channels present many design challenges to engineers developing data acquisition (DAQ) modules and automatic testers for applications such as semiconductor test, memory test, LCD test, and battery test. In these systems, sometimes hundreds or even thousands of data channels are required and thus maximizing SNR performance while minimizing power, component count, and cost are all key design criteria. These systems have some type of power generator that typically includes DC-to-DC converters to provide the voltage levels needed to power each device in the analog front end (AFE). These converters have switching components that cause electromagnetic interference (EMI) emission and harm the system performance.

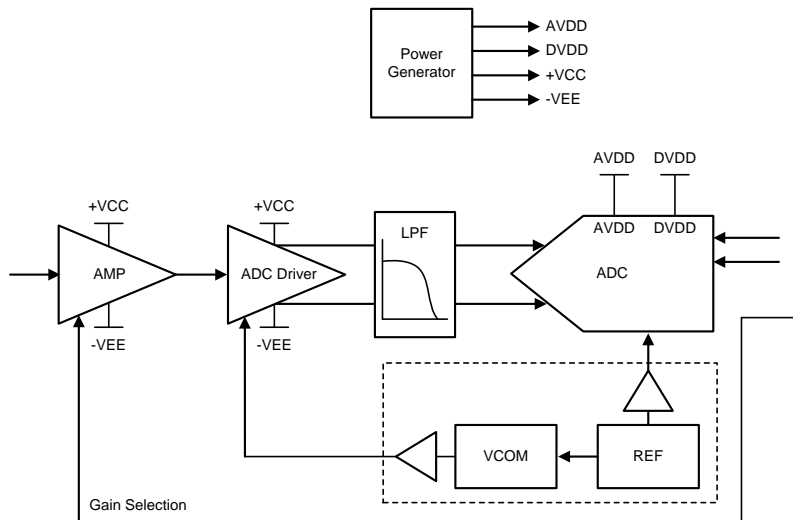


图 1. Generic AFE

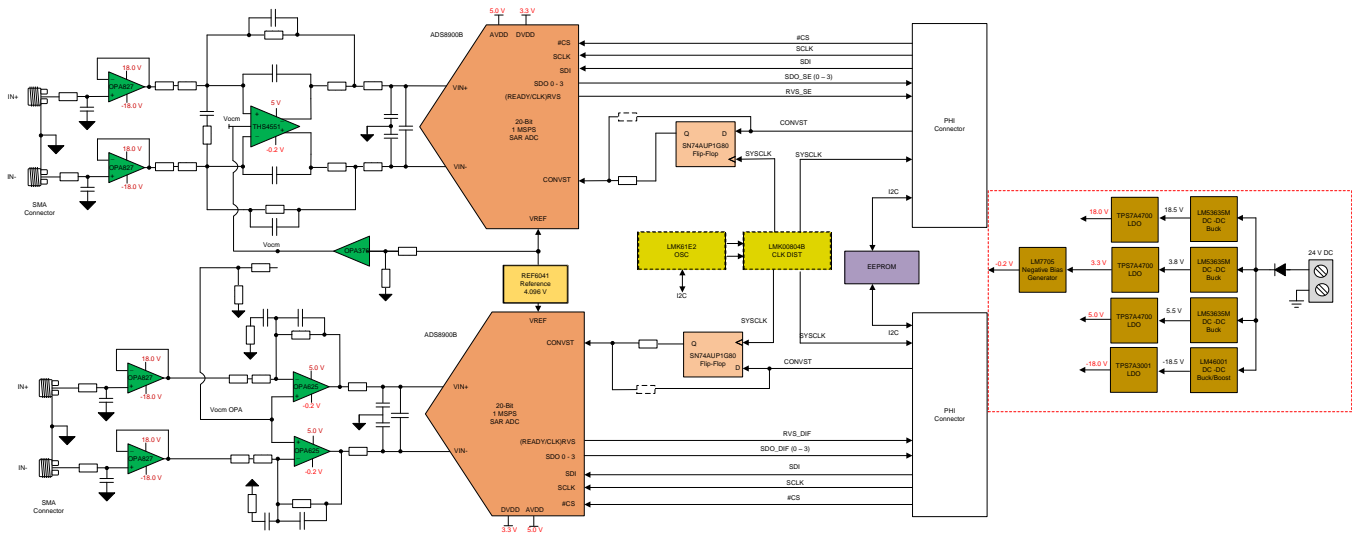
### 1.1 Key System Specifications

表 1. Key System Specifications

PARAMETER	SPECIFICATIONS	MEASURED
Number of channels	Dual	Dual
Input type	Differential	Differential
Input range	8- $V_{pp}$ fully differential	8- $V_{pp}$ fully differential
Resolution	20 bits	20 bits
SNR	> 96 dB	100.13 dB
THD	< -120 dB	-123.06 dB
ENOB	> 16 bit	16.32 bits
System power	< 2.5 W	1.92 W
Form factor (L x W)	120 x 100 mm	112.98 x 99.82 mm

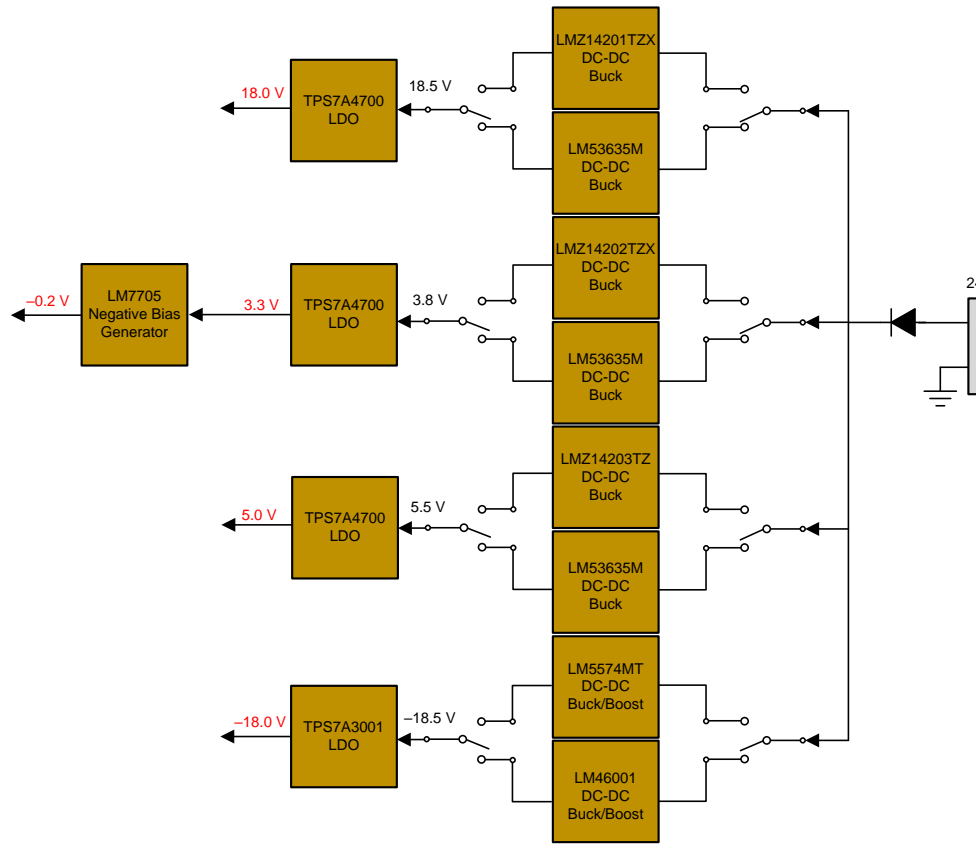
## 2 System Overview

### 2.1 Block Diagram



Copyright © 2017, Texas Instruments Incorporated

图 2. System Block Diagram



Copyright © 2017, Texas Instruments Incorp

图 3. Power Rail Circuitry

This reference design focuses on reducing the EMI generated from the system's buck converters powering the AFE and successive approximation register (SAR) analog-to-digital converter (ADC). This design has two families of buck converters to show the effects of the EMI and solve the issue. [图 3](#) shows how the buck converters can be switched and used in different combinations. The  $-18\text{-V}$  rail has two different buck converters with the LM5574 included for testing purposes only and has no emphasis on the main goal of this reference design: eliminating EMI.

## 2.2 Highlighted Products

### 2.2.1 LM53635-Q1

The LM53635M is used in this design to bring the  $24\text{-V}$  input voltage down to  $3.8\text{ V}$ ,  $5.5\text{ V}$ , and  $18.5\text{ V}$  in a highly efficient manner. This part is selected based on its excellent EMI performance and compact PCB layout. The automotive-qualified HotRod™ QFN package reduces parasitic inductance and resistance while increasing efficiency, minimizing switch node ringing, and dramatically lowering EMI. Seamless transition between pulse-width modulation (PWM) and pulse-frequency modulation (PFM) modes and low quiescent current (only  $15\text{ }\mu\text{A}$  for the  $3.3\text{-V}$  option) ensures high efficiency and superior transient responses at all loads.

## 2.3 System Design Theory

High-performance DAQ systems use high-precision ADC to get the most accurate and precise measurements. These high-resolution ADCs have low-noise floors, which make them more susceptible to the EMI being emitted by DC-to-DC converters. This EMI harms the system performance with spurs that show up throughout the frequency spectrum.

The following sections detail the design challenges for reducing the EMI effects on the SAR ADC performance, including theory, calculations, simulations, PCB layout design, and measurement results. The measurement results outline the difference between the low-EMI LM53635-Q1 buck converter and the easy-to-use LMZ1420x.

### 2.3.1 AFE and SAR ADC

This reference design consists of an AFE with two channels. Both channels are similar with the exception of the ADC driver architecture. The first channel uses the THS4551, a fully differential amplifier specifically designed to be used with high-performance SAR ADCs. The second channel uses dual OPA625 amplifiers wired to work as a fully differential amplifier. These amplifiers are driving the ADS8900B SAR ADC, a 20-bit high-precision and high-speed data converter. The AFE and SAR ADC are key aspects of this design aimed at DAQ systems; however, these devices are not the main focus of this design. To learn more about the design theory of the AFE and SAR ADC, see the [TIDA-01052 reference design](#).

### 2.3.2 Power Structure

This system requires a wide variety of voltage rails to meet the specification of the reference design. The input voltage required for the system is 24-V DC. The power tree in 图 4 highlights the distribution of the power into the different required rails. To create these rails, this design contains the LM53635-Q1 low-EMI buck converter and the LMZ1420x buck converter. These solutions are compared to show the improvement the low-EMI converter has over the popular, easy-to-use LMZ1420x. Using two-pin and three-pin headers allow the user to customize easily which solution to use. See 表 2 for details on using the jumpers. The data gathered for each combination can be found in 3.2 节.

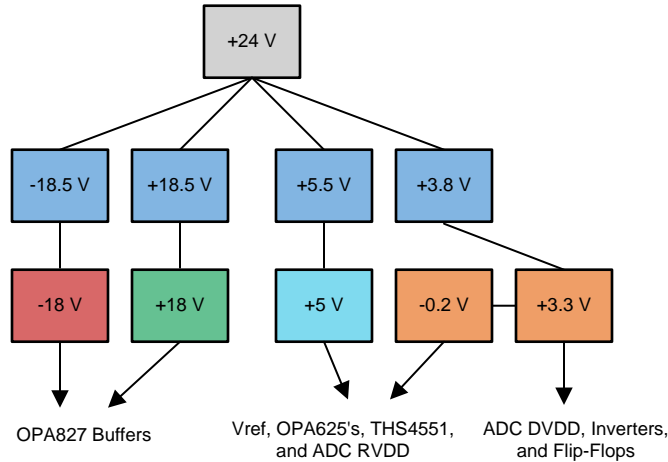


图 4. System Power Tree

#### 2.3.2.1 LM53635-Q1 and LMZ1420x Circuitry

图 5 displays the 18-V rail circuitry with the LM53635-Q1, but each rail is structured the same way with the only difference coming from different passive component values. The input of the buck is connected to the 24-V supply by a two-pin header. This header allows the user to leave unused bucks powered off, which is critical to the testing performed on the reference design. The buck converter is followed by an LDO to remove the switching noise. The input of the LDO is connected to a three-pin header. The other two pins of this header are connected to the outputs of both buck converter options. This header is used in conjunction with the two-pin header to properly connect the buck intended to be used with the LDO. Not only does the three-pin header allow for only one LDO to be used for each rail improving space efficiency, but it also helps with certain aspects of testing and debugging. To get a better visual of the functionality the headers provide, see 图 3.

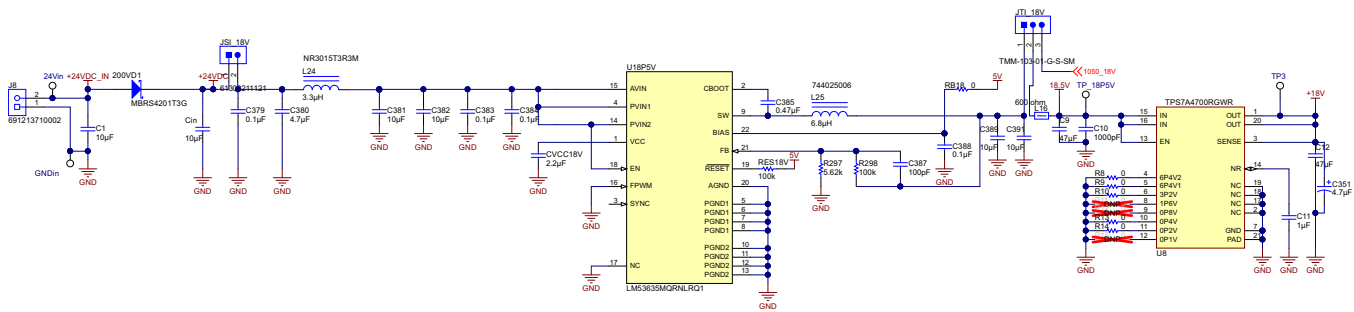
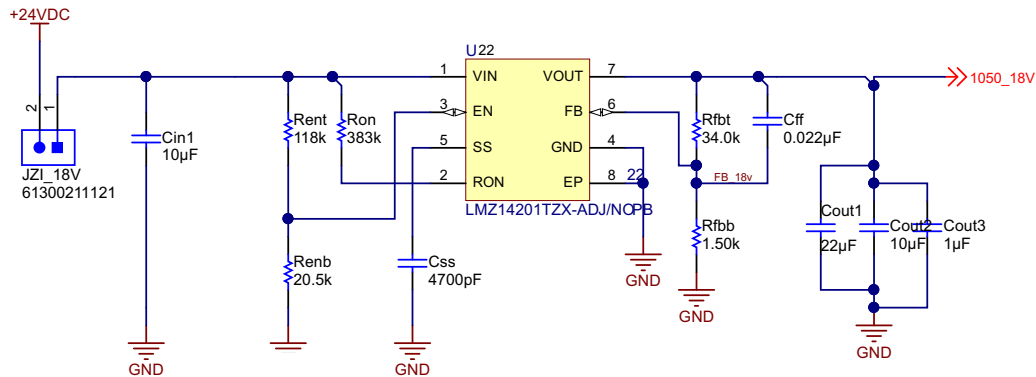


图 5. LM53635-Q1 Schematic

图 6 显示了 LMZ1420x 电路用于 18-V 轨。再次，结构是相同的。输出进入一个板外连接器，该连接器连接到之前讨论过的三针接头。LMZ1420x 降压转换器是模块，因此它们不需要很多额外的被动元件。参见 4.1 节 查看所有电源电路的示意图下载。



Copyright © 2017, Texas Instruments Incorporated

图 6. LMZ1420x Schematic

### 2.3.3 LM53635-Q1 Switching Noise

降压转换器开关元件会产生输出电压纹波，这被称为开关噪声。纹波的幅度由许多与开关调节器相关的不同因素决定，可能高到足以导致由该降压转换器供电的设备出现问题。当涉及到对噪声敏感的设备，如本参考设计中使用的 20 位 ADC 时，高压纹波可能会对信号完整性产生非常有害的影响。为了克服这一点，在开关调节器的输出端放置一个 LDO 以消除开关噪声。

以下计算和仿真说明了让 LDO 消除开关频率的重要性。降压转换器在 5-V 轨（为 ADC 的 RVDD 供电的轨）的输出电压纹波计算为大约 30 mV，使用公式 1：

$$\Delta V = \frac{I_L \times (\Delta I - I_L)^2}{C \times f_S \times \Delta I^2} \quad (1)$$

公式 1 用于在断续导通模式 (DCM) 中的降压转换器。LM53635-Q1 在连续导通模式 (CCM) 和 DCM 之间切换，当负载电流低于 148-mA 阈值时。负载电流 ( $I_L$ ) 测量为 22 mA，因此使用公式 1。因为降压转换器在此设计中配置为自动模式，所以在轻载条件下，降压转换器会从 PWM 切换到 PFM。这意味着降压转换器会调整其开关频率以调节输出。因此，开关频率远低于在 LM53635-Q1 数据表中找到的典型 2.1 MHz。开关频率 ( $f_S$ ) 测量为 15.708 kHz。降压转换器设计为输出 5.5 V，刚好高于 LDO 的 dropout 电压，以最大限度地减少效率损失。为 TPS7A4700 LDO 创建了一个 TINA-TI™ 仿真模型，具有 5.5 V 的阶跃输入和 30 mVpk-pk 的正弦波输入（模拟降压转换器的输出纹波）。稳态分析给出了 LDO 的输出，如图 7 所示。

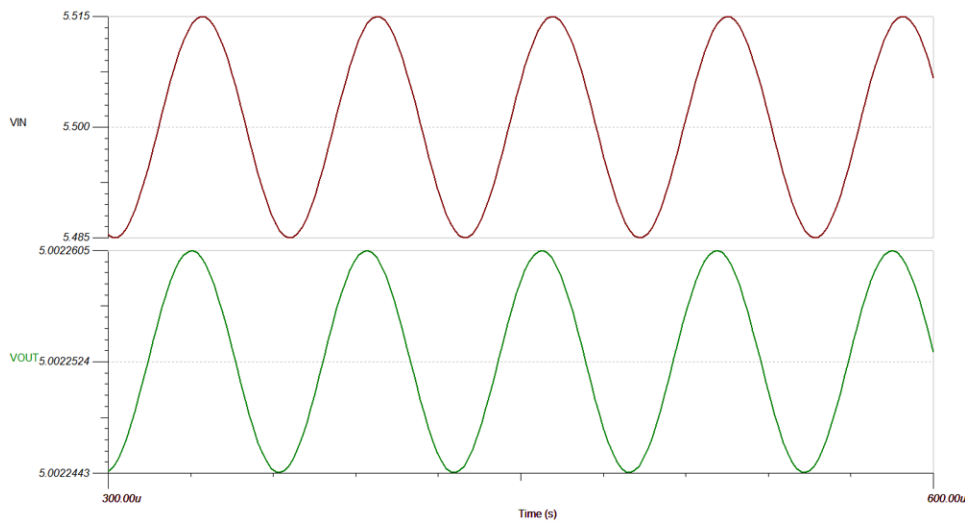


图 7. TPS7A47 LDO Simulation for 5-V Rail

After the LDO, the peak-to-peak amplitude of the switching noise is 16.2  $\mu\text{V}$ . The LDO effectively reduced the switching ripple noise by a factor of 1850. Further calculations are made to see the noise present at the ADC using the output voltage ripple of the LM53635-Q1. This result is compared to the result of using the output voltage ripple of the TPS7A4700 in the same calculations. This ripple voltage without the LDO goes to both the OPA625 and the THS4551. The THS4551 has a PSRR of 110 dB at 15.708 kHz and a gain of 1. PSRR is equal to:

$$\text{PSRR}(\text{dB}) = -20 \log_{10} \left( \frac{\Delta V_{\text{OS}}}{\Delta V_{\text{SUPPLY}}} \right) \quad (2)$$

Because this system has a gain of 1, the total noise gain on the non-inverting terminal is 1 + 1. This is a gain of 6 dB. The total PSRR for the THS4551 is approximately 104 dB for this system. This value is equal to 0.00000631 V/V. The amount of power supply noise coupled to the ADC data lines is calculated using 公式 3:

$$30 \text{ mV} \times 0.00000631 = 189.3 \text{ nV} \quad (3)$$

This noise value is then compared to the LSB value of the ADC to observe the effect it has on signal integrity. The value of 1 LSB for a differential input, 20-bit ADC with 4.096 V as a reference voltage is found using 公式 4 and 公式 5:

$$\frac{2 \times 4.096}{2^{20}} = 7.812 \mu\text{V} \quad (4)$$

$$\frac{189.3 \text{ nV}}{7.812 \mu\text{V}} \times 100 = 2.42\% \text{ LSB} \quad (5)$$

The OPA625 has a power supply rejection ratio of 86 dB at 15.708 kHz. At a gain of 1, the PSRR is equal to 80 dB. This value is equivalent to 0.0001 V/V. The power supply noise present at the ADC driven by the OPA625 is:

$$30 \text{ mV} \times 0.0001 = 3 \mu\text{V} \quad (6)$$

$$\frac{3 \mu\text{V}}{7.812 \mu\text{V}} \times 100 = 38.4\% \text{ LSB} \quad (7)$$

With 2.42% LSB present at the ADC, the THS4551 signal chain is not greatly impacted by excluding the LDO. However, the OPA625 signal chain has a little less than 50% LSB of power supply noise present at the ADC without the LDO. Thus, it can have a negative impact on the output data of the ADC. Using the LDO's output ripple of 16.2  $\mu\text{V}$  and the same equations, the amount of power supply noise coupled to the ADC data lines for the ADC driven by the THS4551 is:

$$16.2 \mu\text{V} \times 0.00000631 = 102.2 \text{ pV} \tag{8}$$

$$\frac{102.2 \text{ pV}}{7.812 \mu\text{V}} \times 100 = 0.0013\% \text{ LSB} \tag{9}$$

This highlights that the amount of noise on the 5-V rail is much less than 1% of the LSB value of the ADC. The amount of power supply noise present at the ADC of the OPA625 is:

$$16.2 \mu\text{V} \times 0.0001 = 1.62 \text{ nV} \tag{10}$$

$$\frac{1.62 \text{ nV}}{7.812 \mu\text{V}} \times 100 = 0.021\% \text{ LSB} \tag{11}$$

When using the LDO, both the THS4551 and OPA625 signal chain ADCs have much less than 1% LSB of noise present at their power supply inputs. This guarantees that there is no negative impact on signal integrity with the LDO present in the system. This concludes that the LDO is necessary in the power rail circuits to overall remove any system performance degradation due to switching noise.

### 2.3.4 LM53635-Q1 EMI

One of the goals for this design is to eliminate any system performance degradation due to EMI for high-performance DAQ systems. Because buck converters have harsh switching components, they are the main culprit in producing unwanted spurs throughout the spectrum. The LM53635-Q1 is a great solution for this problem with its many features focused on reducing EMI.

#### 2.3.4.1 HotRod Packaging

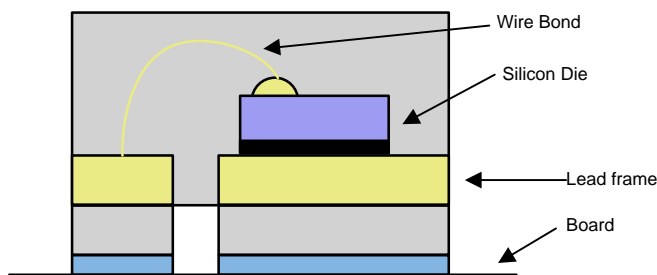


图 8. Standard Wire Bond QFN

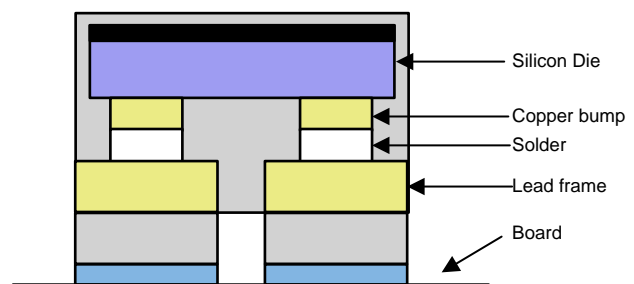


图 9. HotRod FCOL QFN

The biggest factor that helps the LM53635-Q1 reduce EMI is the HotRod FCOL packaging illustrated in 图 9. This package style flips the die over and uses copper bumps to connect directly to the leads, removing the need for a wire bond seen in 图 8. By removing this wire bond, the parasitics are reduced, which dramatically lowers the switch node ringing. This ringing is a major source of EMI for buck converters using the standard wire bond packaging.

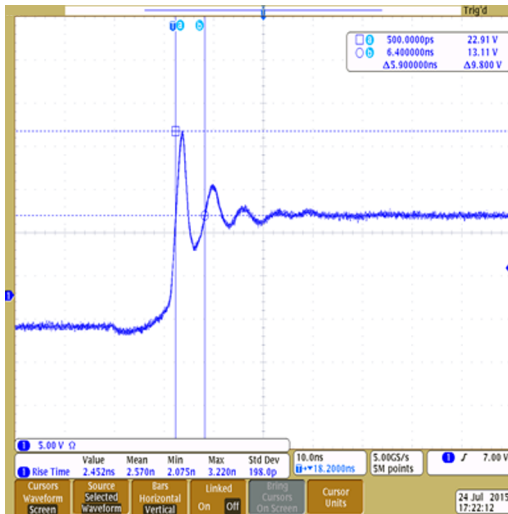


图 10. LM53603 TSSOP

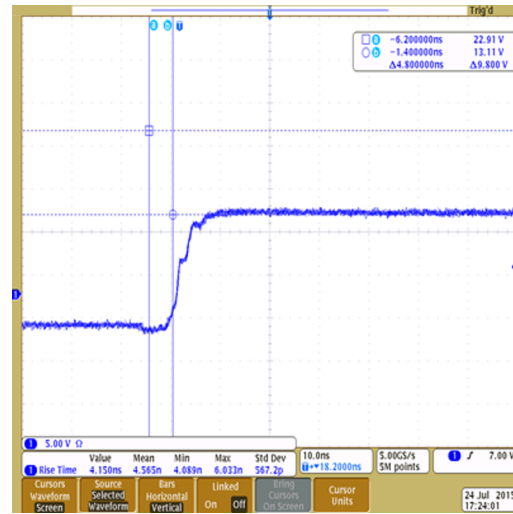


图 11. LM53635-Q1 FCOL

The difference between switch node ringing for a wire bond package and a HotRod package is illustrated in 图 10 and 图 11. The ringing overshoot is reduced from 9 V to 0 V, lowering the overall EMI and noise. Not only does the HotRod packaging help reduce EMI, but it also allows for a smaller size and reduced  $R_{DS\_ON}$ , improving efficiency.

### 2.3.4.2 Spread Spectrum

The LM53635-Q1 has an option with spread spectrum capabilities, which is used in this reference design. Spread spectrum is a means of reducing EMI by dithering the switching regulator frequency. This causes the noise power to spread over a wider frequency band and reduces the fundamental energy. Most systems containing the LM53635-Q1 device can easily filter low-frequency conducted emissions from the first few harmonics of the switching frequency. A more difficult design criterion is reducing emissions at higher harmonics, which fall in the FM band. These harmonics often couple to the environment through electric fields around the switch node. The LM53635-Q1 device uses a  $\pm 3\%$  spread of frequencies, which spreads energy smoothly across the FM band but is small enough to limit sub-harmonic emissions below its switching frequency. Peak emissions at the switching frequency of the LM53635-Q1 are only reduced by slightly less than 1 dB, while peaks in the FM band are typically reduced by more than 6 dB, which can be seen in 图 12 and 图 13.

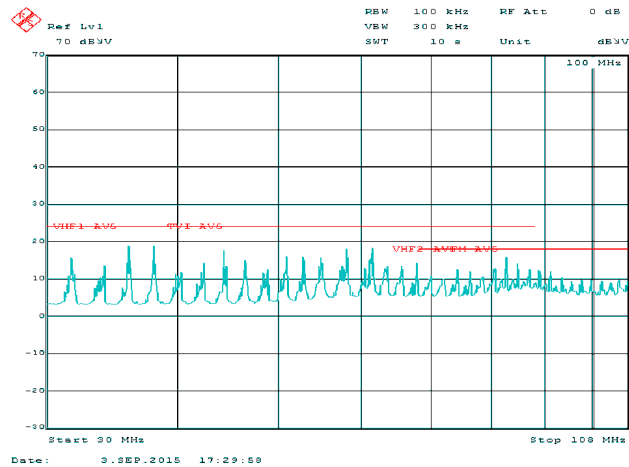


图 12. 30 to 108 MHz Without Spread Spectrum

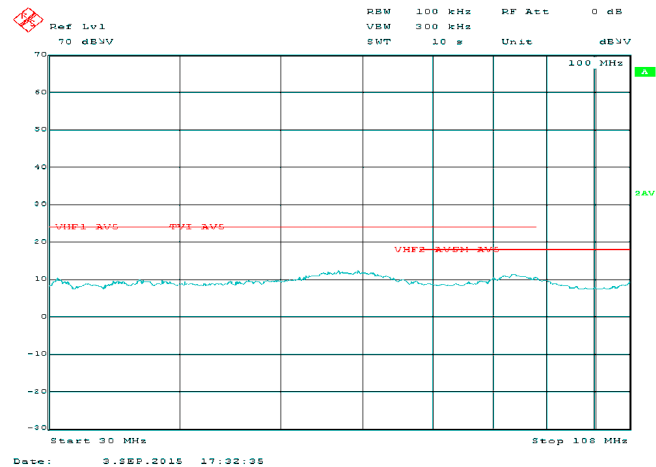


图 13. 30 to 108 MHz With Spread Spectrum

The LM53635-Q1 uses a cycle-to-cycle frequency hopping method based on a linear feedback shift register. An intelligent pseudo-random generator limits cycle-to-cycle frequency changes to limit output ripple. The pseudo-random pattern repeats by approximately 8 Hz, which is below the audio band.

### 3 Hardware, Software, Testing Requirements, and Test Results

#### 3.1 Required Hardware

The ensuing section outlines the information for getting the board up and running as fast as possible. To learn about the PHI board or the onboard clocking and jitter cleaner, see the [TIDA-01050 reference design](#). Take care when moving jumper pins to avoid possible damage to the components.

##### 3.1.1 Jumper Configuration

This system has several configurable power options. These options are selectable through using two-pin and three-pin jumpers. [表 2](#) highlights the purpose of each jumper and assists in changing the configuration to fit the needs of the user.

**表 2. Jumper Configuration**

JUMPER NAME	SHORT PINS 1 AND 2	SHORT PINS 2 AND 3	DEFAULT CONFIGURATION
JSI_18V	Power to LM53635-Q1 18-V rail	—	Short
JTI_18V	Connects LM53635-Q1 to TPS7A700 for 18-V rail	Connects LMZ14201 to TPS7A700 for 18-V rail	Short pins 1 and 2
JSI_5V	Power to LM53635-Q1 5-V rail	—	Short
JTI_5V	Connects LM53635-Q1 to TPS7A700 for 5-V rail	Connects LMZ14203 to TPS7A700 for 5-V rail	Short pins 1 and 2
JSI_3.3V	Power to LM53635-Q1 3.3-V rail	—	Short
JTI_3.3V	Connects LM53635-Q1 to TPS7A700 for 3.3-V rail	Connects LMZ14202 to TPS7A700 for 3.3-V rail	Short pins 1 and 2
JPRI_–18V	Power to LM46001 –18-V rail	—	Short
JTI_–18V	Connects LM46001 to TPS7A3001 for –18-V rail	Connects LM5574 to TPS7A3001 for –18-V rail	Short pins 1 and 2
JMTI_–18V	Power to LM5574 –18-V rail	—	Open
JZI_18V	Power to LMZ14201 18-V rail	—	Open
JZI_3.3V	Power to LMZ14202 3.3-V rail	—	Open
JZI_5V	Power to LMZ14203 5-V rail	—	Open
J39	Connects –0.2-V rail to OPA 625 and THS4551	Shorts –0.2-V rail to ground	Short pins 1 and 2

## 3.2 Testing and Results

An Audio Precision 2700 series signal generator is used as the signal source to test the AFE and ADC performance. The noise and THD of the AP2700 have adequate performance and do not limit measurements or system performance. A generic DC power supply is used to generate the 24-V DC input voltage.

A PHI controller board is used to connect the TIDA-01054 board to the host PC, where the ADS8900B EVM GUI is being run. This software allows for measuring SNR, THD, SFDR, SINAD, and ENOB for the ADC by running a spectral analysis. The AP2700 is set to output a 2-kHz 8-Vpk-pk sinusoid. 2 kHz is chosen because it is the standard frequency when measuring noise and THD, and 8-Vpk-pk grants full range on the THS4551 or OPA625, thus granting full range of 0 to VREF for the ADC.

### 3.2.1 EMI Matters

This reference design focuses on how EMI generated by switching regulators affects the system performance of high-performance DAQs. To illustrate this, a test is run to demonstrate the effects of EMI using two TIDA-01054 boards: one connected to the PC and AP2700 and the other providing power. [图 14](#) displays the physical setup.

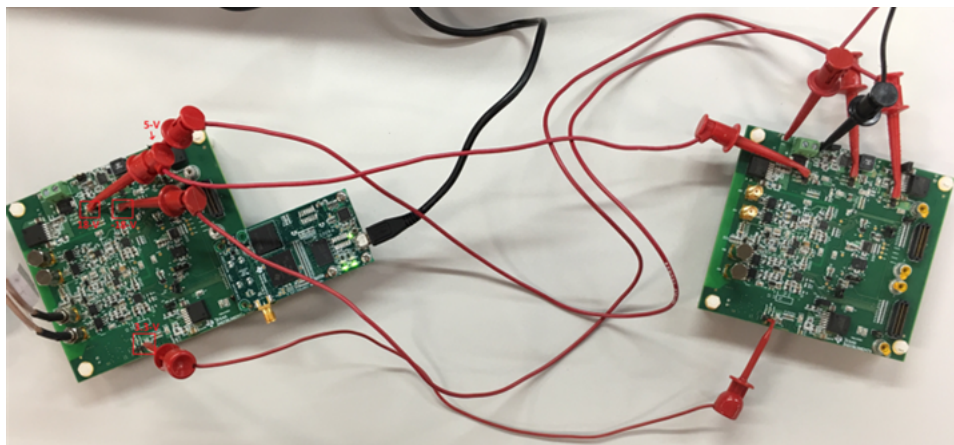


**图 14. Physical Setup for EMI Testing**

The board on the left of [图 14](#) is the board under test and on the right is the board providing power. The power board is set up to use all LMZ1420x and LM46001 buck converters because it is the theoretical worst case scenario. The outputs of these bucks are being connected to the inputs of the LDOs on the board under test. Thus, whenever an external source is referenced, it is coming from this board. [图 15](#) and [图 16](#) illustrate the performance difference between using the external power board and the onboard LMZ1420x and LM46001 buck converters.

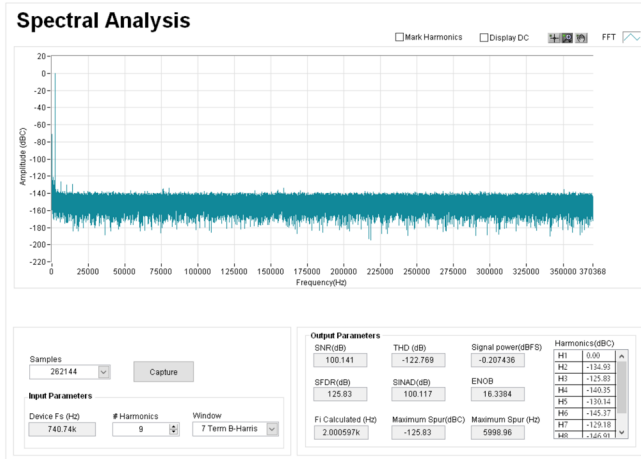


图 15. EMI Test With External Power

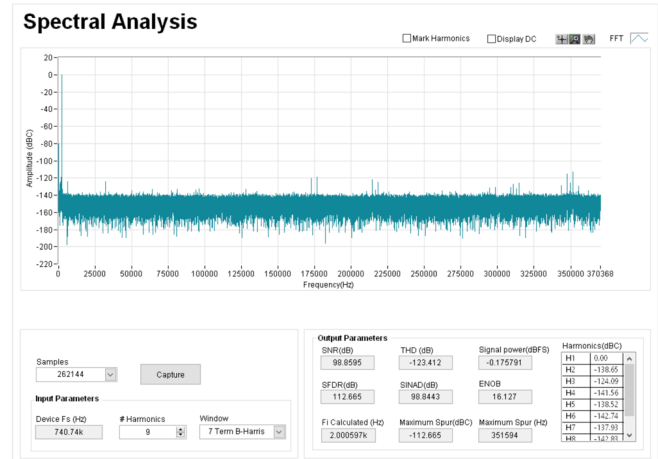


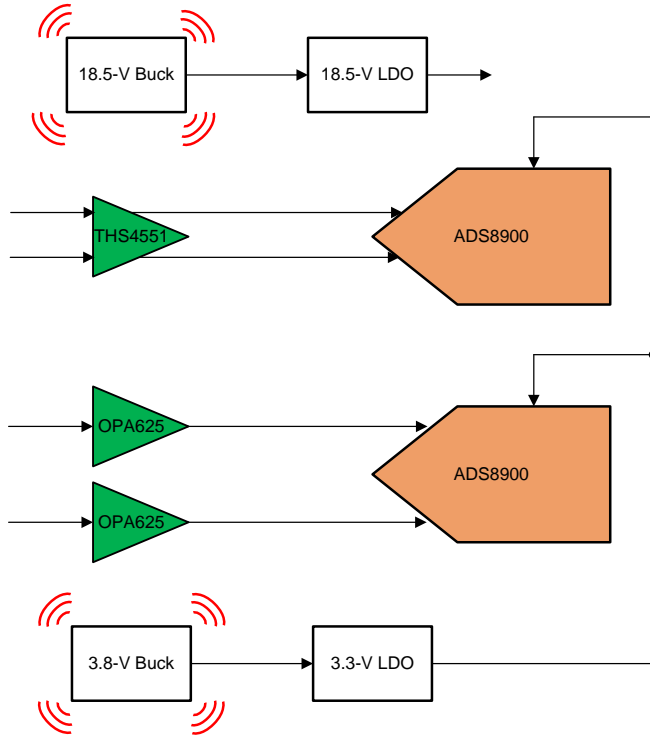
图 16. EMI Test With Onboard Power

The measured results are taken from the top channel of the design. It is very apparent looking at the spectrum plot that the system performance degrades when using onboard power. Spurs show up at multiple frequencies with some having an amplitude up to  $-112$  dBc. These spurs are narrow so they do not affect the SNR as much as the SFDR, but both decrease considerably with the SFDR dropping roughly 13 dB. Because both boards are using the same buck converters, the conclusion can be made that EMI is the cause of the poor performance. With roughly one foot of space between the board under test and the power board, the radiated EMI from the switching components of the bucks are not introduced into the input signal.

### 3.2.2 Proximity and $\Delta V$ Factor in EMI Degradation

The proximity and  $\Delta V$  of the buck converter are major factors in the EMI impact on system performance. However, these factors are mitigated with the LM53635-Q1. To prove this, the LM53635-Q1 outputting 3.8 V (making it the highest  $\Delta V$ ) is swapped with the LM53635-Q1 outputting 18.5 V to change the proximity to both channels. 图 17 and 图 19 are diagrams to simplify this process. With the highest  $\Delta V$  buck placed close to the differential channel, the system performance is measured to observe the effects.

图 18 displays the spectrum results of the differential channel when the two bucks are in their original positions, referred to as position 1. Compared the results of position 2 in 图 20, the system performance stayed the same. With no degradation in system performance, the LM53635-Q1 effectively eliminates EMI and presents no concern with the proximity of this buck, even with high  $\Delta V$ .



Copyright © 2017, Texas Instruments Incorporated

图 17. Position 1

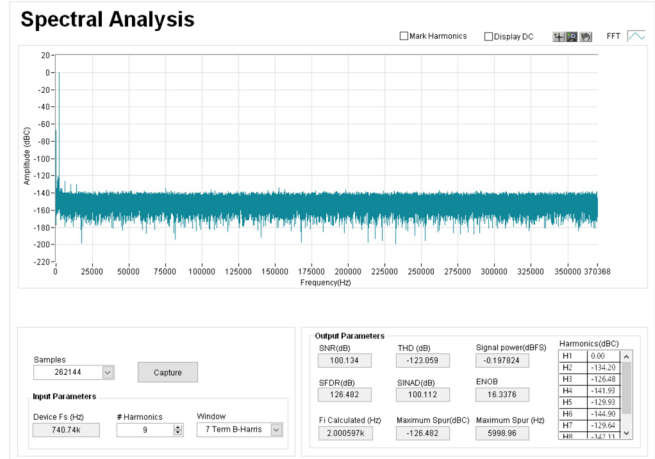
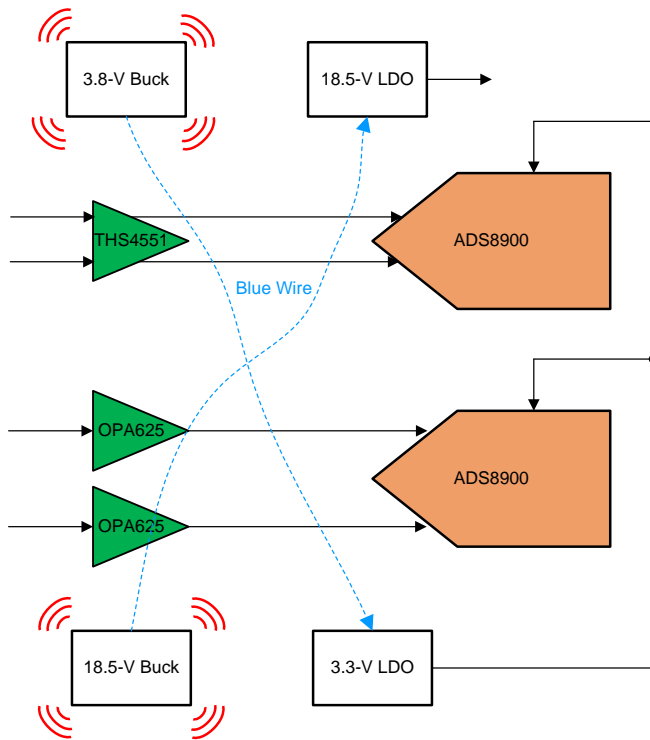


图 18. Spectrum Results for Position 1



Copyright © 2017, Texas Instruments Incorporated

图 19. Position 2

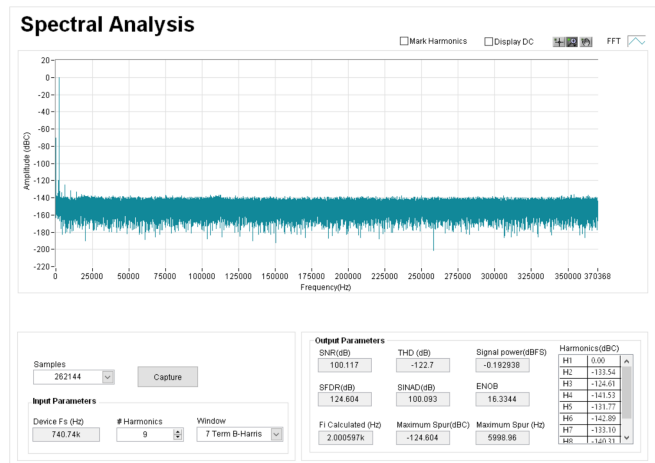


图 20. Spectrum Results for Position 2

### 3.2.3 Buck Converter and ADC Driver Comparison

This reference design contains two options for power and for driving the ADC. These options allow for a comparison of performance to see which option is better overall. It is expected that the THS4551 amplifier, used in the differential channel, is a better ADC driver over the dual OPA625 amplifiers, used in the single-ended channel, because the system's bandwidth is limited to the frequency range, where its noise performance is superior. It is also expected that the LM53635-Q1 grants better performance over the LMZ1420x due to its emphasis on low EMI and HotRod packaging. To perform the tests, measurements are taken from each channel separately while also alternating the LM53635-Q1 and LMZ1420x buck converters to power the rails. The results are highlighted in [表 3](#).

**表 3. Summary of Measured Results**

3.8-V BUCK POSITION	VOLTAGE SOURCE	ADC CHANNEL	SNR (dB)	SINAD (dB)	THD (dB)	SFDR (dB)	ENOB (bits)
Position 1	LMZ1420x	Differential	98.86	98.84	-123.41	112.67	16.13
Position 1	LM53635-Q1	Differential	100.13	100.11	-123.06	126.48	16.34
Position 2	LM53635-Q1	Differential	100.12	100.09	-122.70	124.60	16.33
—	External	Differential	100.14	100.12	-122.77	126.55	16.34
Position 1	LM53635-Q1	Single-ended	98.57	98.56	-129.55	131.98	16.08
Position 2	LM53635-Q1	Single-ended	98.82	98.82	-129.10	131.61	16.12
—	External	Single-ended	99.45	99.45	-129.70	132.22	16.23

When comparing the differential channel (THS4551) and the dual single-ended channel (OPA625), external power sources are used to isolate performance specifically to the devices themselves. As expected, the THS4551 outperformed the OPA625 by almost 1 dB in SNR. With that, most of the results are taken from the differential channel to get the best overall performance with the buck converters. When using the LM53635-Q1 devices over the LMZ1420x, the SNR performance improved slightly over 1 dB. The SFDR improved by roughly 14 dB because the spurs caused by EMI are very narrow so they do not have a major impact on the total noise even though they have high amplitudes. The single-ended results are added in [表 3](#) to emphasize the better rejection to EMI noise the THS4551 has over the two OPA625 amplifiers. The column named "3.8-V Buck Position" refers to the testing done in [节 3.2.2](#).

All the tests performed help solidify that EMI, with impacting factors of  $\Delta V$  and proximity, does matter in high-performance DAQ systems. The lower noise floor of a 20-bit SAR ADC makes the spurs caused by the switching components of the buck converters more prominent. With the LM53635-Q1 achieving low EMI, this issue is solved and the system performance degradation is greatly reduced, which is illustrated in [图 21](#) and [图 22](#). The LMZ1420x is a widely used buck converter because of its ease of use, but the LM53635-Q1 is a far superior option if the user wants to design a system with a high-resolution ADC. With this option, the user can include power on the same board as the sensitive signal chain with no concern to proximity and still get the same performance as with an external power source.

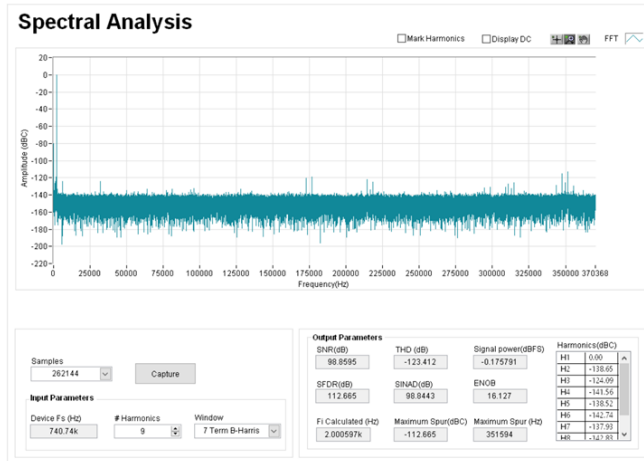


图 21. Spectral Results for LMZ1420x

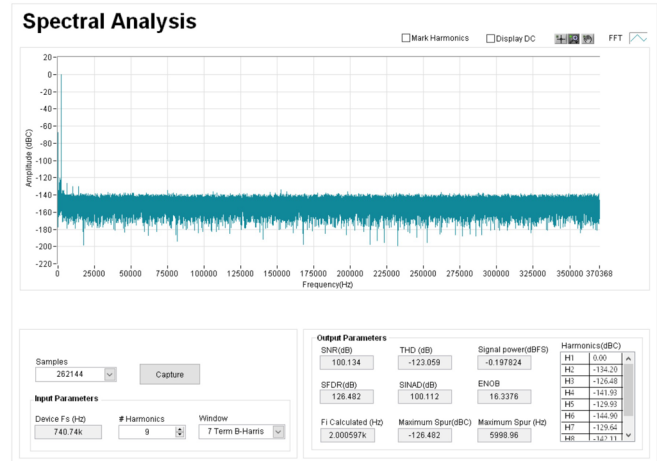


图 22. Spectral Results for LM53635-Q1

## 4 Design Files

### 4.1 Schematics

To download the schematics, see the design files at [TIDA-01054](#).

### 4.2 Bill of Materials

To download the bill of materials (BOM), see the design files at [TIDA-01054](#).

### 4.3 PCB Layout Recommendations

The LM53635-Q1 has certain layout guidelines that help it cut down on EMI. 图 23 illustrates how the LM53635-Q1 and its additional components must be placed in the layout.

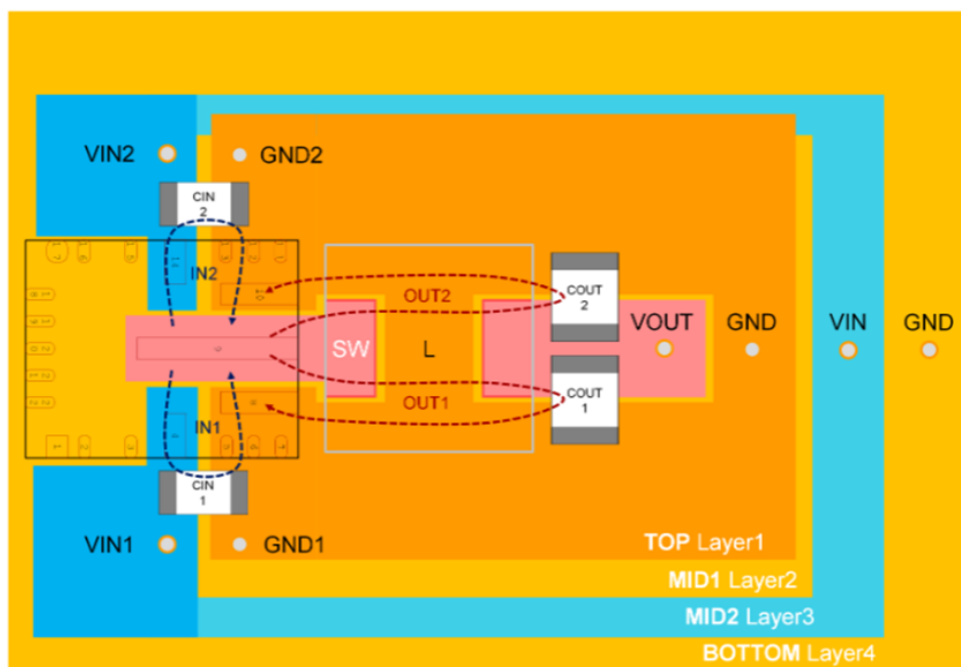


图 23. LM53635-Q1 Layout Guidelines

Putting the input and output capacitors in this configuration creates parallel capacitance loops, minimizing the inductance. This placement then reduces the switch node ringing and overall lowers the EMI emissions. Another recommendation is to leave the ground plane unbroken under the device. This provides the shortest return path possible, minimizing EMI generated by the loop. For more layout recommendations regarding the AFE or SAR ADC, see the [TIDA-01050 reference design](#).

#### 4.3.1 Layout Prints

To download the layer plots, see the design files at [TIDA-01054](#).

### 4.4 Altium Project

To download the Altium project files, see the design files at [TIDA-01054](#).

## 4.5 Gerber Files

To download the Gerber files, see the design files at [TIDA-01054](#).

## 4.6 Assembly Drawings

To download the assembly drawings, see the design files at [TIDA-01054](#).

## 5 Software Files

To download the software files, see the design files at [TIDA-01054](#).

## 6 Related Documentation

1. Texas Instruments, [TIDA-01052 ADC Driver Reference Design Improving Full Scale THD Using Negative Supply Design Guide](#)

### 6.1 商标

E2E, HotRod, TINA-TI are trademarks of Texas Instruments.  
All other trademarks are the property of their respective owners.

## 7 About the Authors

**DYLAN HUBBARD** is a systems engineer at Texas Instruments, where he is responsible for developing reference design solutions for the test and measurement industry. Dylan obtained his bachelor's degree from Texas A&M University in Electronic Systems Engineering Technology (ESET).

**TARAS DUDAR** is a systems design engineer and architect at Texas Instruments, where he is responsible for developing reference design solutions for the test and measurement industry. Previously, Taras designed high-speed analog SOC integrated circuits for Gbps data communications. Taras has earned his master of science in electrical engineering (MSEE) degree from the Oregon State University in Corvallis, OR.

## 修订历史记录

注：之前版本的页码可能与当前版本有所不同。

<b>Changes from Original (September 2017) to A Revision</b>	<b>Page</b>
• Corrected LM53635 part number in Figure 5: <i>LM53635-Q1 Schematic</i> .....	5
• Updated Equation 4 .....	7
• Updated Equation 5 .....	7
• Updated Equation 7 .....	7
• 已更改 the amount of LSB present at the ADC from 4.85% to 2.42% .....	8
• 已更改 the amount of noise the OPA625 has at the ADC from 1 LSB to 50% .....	8
• Updated Equation 9 .....	8
• Updated Equation 11 .....	8

## 有关 TI 设计信息和资源的重要通知

德州仪器 (TI) 公司提供的技术、应用或其他设计建议、服务或信息，包括但不限于与评估模块有关的参考设计和材料（总称“TI 资源”），旨在帮助设计人员开发整合了 TI 产品的应用；如果您（个人，或如果是代表贵公司，则为贵公司）以任何方式下载、访问或使用了任何特定的 TI 资源，即表示贵方同意仅为该等目标，按照本通知的条款进行使用。

TI 所提供的 TI 资源，并未扩大或以其他方式修改 TI 对 TI 产品的公开适用的质保及质保免责声明；也未导致 TI 承担任何额外的义务或责任。TI 有权对其 TI 资源进行纠正、增强、改进和其他修改。

您理解并同意，在设计应用时应自行实施独立的分析、评价和判断，且应全权负责并确保应用的安全性，以及您的应用（包括应用中使用的 TI 产品）应符合所有适用的法律法规及其他相关要求。就您的应用声明，您具备制订和实施下列保障措施所需的一切必要专业知识，能够 (1) 预见故障的危险后果，(2) 监视故障及其后果，以及 (3) 降低可能导致危险的故障几率并采取适当措施。您同意，在使用或分发包含 TI 产品的任何应用前，您将彻底测试该等应用和该等应用所用 TI 产品的功能而设计。除特定 TI 资源的公开文档中明确列出的测试外，TI 未进行任何其他测试。

您只有在为开发包含该等 TI 资源所列 TI 产品的应用时，才被授权使用、复制和修改任何相关单项 TI 资源。但并未依据禁止反言原则或其他法律授予您任何 TI 知识产权的任何其他明示或默示的许可，也未授予您 TI 或第三方的任何技术或知识产权的许可，该等许可包括但不限于任何专利权、版权、屏蔽作品权或与使用 TI 产品或服务的任何整合、机器制作、流程相关的其他知识产权。涉及或参考了第三方产品或服务的信息不构成使用此类产品或服务的许可或与其相关的保证或认可。使用 TI 资源可能需要您向第三方获得对该等第三方专利或其他知识产权的许可。

TI 资源系“按原样”提供。TI 兹免除对 TI 资源及其使用作出所有其他明确或默示的保证或陈述，包括但不限于对准确性或完整性、产权保证、无复发故障保证，以及适销性、适合特定用途和不侵犯任何第三方知识产权的任何默认保证。

TI 不负责任何申索，包括但不限于因组合产品所致或与之有关的申索，也不为您辩护或赔偿，即使该等产品组合已列于 TI 资源或其他地方。对因 TI 资源或其使用引起或与之有关的任何实际的、直接的、特殊的、附带的、间接的、惩罚性的、偶发的、从属或惩戒性损害赔偿，不管 TI 是否获悉可能会产生上述损害赔偿，TI 概不负责。

您同意向 TI 及其代表全额赔偿因您不遵守本通知条款和条件而引起的任何损害、费用、损失和/或责任。

本通知适用于 TI 资源。另有其他条款适用于某些类型的材料、TI 产品和服务的使用和采购。这些条款包括但不限于适用于 TI 的半导体产品 (<http://www.ti.com/sc/docs/stdterms.htm>)、[评估模块](http://www.ti.com/sc/docs/sampters.htm)和样品 (<http://www.ti.com/sc/docs/sampters.htm>) 的标准条款。

邮寄地址：上海市浦东新区世纪大道 1568 号中建大厦 32 楼，邮政编码：200122  
Copyright © 2018 德州仪器半导体技术（上海）有限公司